UDC 551.584.5:551.524.31:551.511.36

A Study of the Atmospheric Response Due to a Diurnal Heating Function Characteristic Of an Urban Complex

FRED M. VUKOVICH—*Research Triangle Institute, Research Triangle Park, N.C.*

ABSTRACT—The variation of the differential heating required to depict the diurnal behavior of the urban heat island is established from temperature data obtained in the literature and from other sources. A simple, linear, three-layer model was developed to study the response of the urban atmosphere to the differential heating in the no-mean-wind case. The only driving force in the model was differential heating. The solutions suggest that the urban atmosphere experiences a short period of upward vertical motion in the early evening (the urban heat island circulation) in response to the positive differential heating at this time and a short period of downward vertical motion in the late morning in response to the negative differential heating at that time. The latter response would prevent diffusion of pollutants in the vertical and would bring an elevated pollution layer over the city to the surface. Therefore, the dynamic response could be responsible for the production of a "critical episode" in the city.

1. INTRODUCTION

It has been well established that the difference in temperature between a city and its surrounding environment attains a maximum value at night and that the city is warmer (Landsberg 1956, Chandler 1964, 1965, 1967, Woollum 1964, Woollum and Canfield 1968). The effect is called the urban heat island. Temperature differences as large as 8°C have been demonstrated (Peterson 1969, Mitchell 1961, Chandler 1965), and differences of 4°–6°C are common for large cities. In the daytime, the temperature difference is a minimum or, in some cases, becomes negative (i.e., the environment is warmer than the city) (Mitchell 1961, Landsberg 1956, Ludwig 1967, Peterson 1969); most often, however, the temperature difference is zero.

Figures 1, 2, and 3, respectively, demonstrate the diurnal variations of the urban heat island for Vienna, Austria, St. Louis, Mo., and San Francisco, Calif., in the winter and summer. The Vienna data are average data for the month. The St. Louis and San Francisco data represent days of clear sky and low wind speed. The figures show that around 1500–1600 LST the differences in the cooling rates between the city and the suburbs produce a temperature difference, and the city is warmer. The temperature difference increases through the late afternoon, early evening, and night, and attains a maximum just before sunrise. In the summer, the differential cooling rate can be attributed mainly to radiation processes. The multiple reflection and absorption of radiant energy in the structural regions of the city allow the city to maintain heat for longer periods than in the suburbs (Lowry 1967). Also, the shroud of air pollutants that hovers over the city would absorb the long-wave radiation from the city, and radiant heat energy would be emitted from the pollution layer to the city (Atwater 1971*a*). In the winter, radiation processes are also important, but artificial heat sources in the city (e.g., combustion from home heating) play a significant role.

After sunrise, the temperature difference is minimized quickly in all cases. About 15–16 hr after initiation, the urban heat island attains its maximum intensity, but the temperature difference is reduced to zero, or minimized to a small fraction of its maximum value, in less than one-half the time it takes to produce the maximum. The magnitude of the differential heating rate after sunrise must be two to four times greater than that associated with the production of the heat island to accomplish this. This behavior is also evident in the data presented by Hage (1972) and Ackerman and Wormington (1971).

The difference in heating rates after sunrise can be attributed to the shroud of air pollution over the city and to surface albedo. Atwater (1971*a*) indicates that much of the solar energy is either reflected back to space or is absorbed by the air pollutants. These effects are most pronounced where the air pollution concentration is largest and are negligible in the surrounding environment compared to the city since the pollution concentrations would be smaller in the no-mean-wind case. Thus, the suburbs will heat more rapidly.

Figure 4 shows the diurnal variation of a function, $F(t)$, which is defined as the ratio between the differential heating at any hour to the maximum positive differential heating. The differential heating is defined as the difference between the heating rate in the city (proportional to the local rate of change of temperature in the city) and the rate in the suburbs (proportional to the local rate of change of temperature in the suburbs) and is positive if

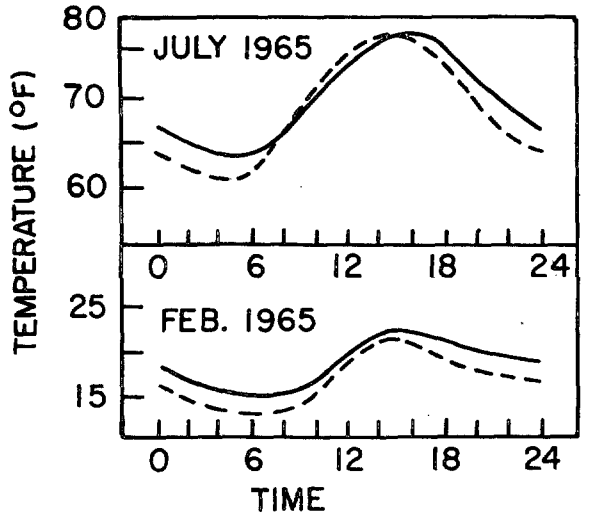

FIGURE 1.—Diurnal (LST) variation of temperature in the city of Vienna, Austria, (solid line) and a neighboring suburban station (dashed line) for the summer (July) and winter (February) cases (Mitchell 1962).

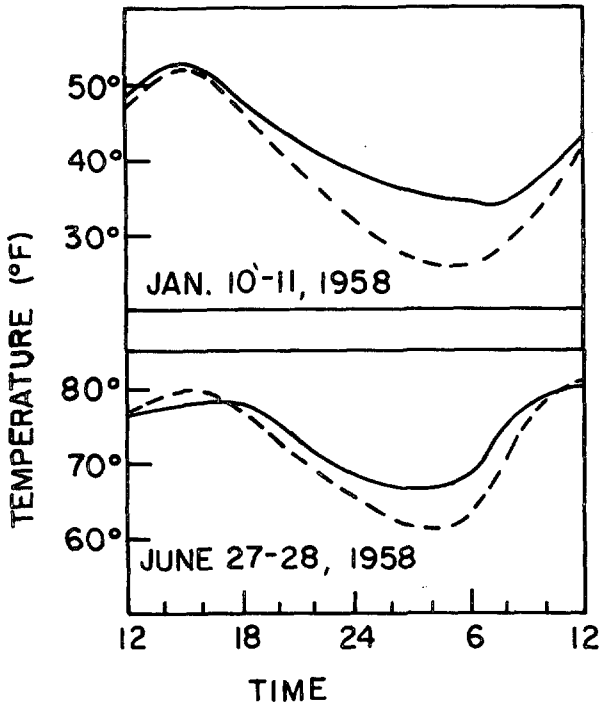

FIGURE 2.—Diurnal (LST) variation of the temperature in the city of St. Louis, Mo., (solid line) and at the airport (dashed line). These data have been filtered.

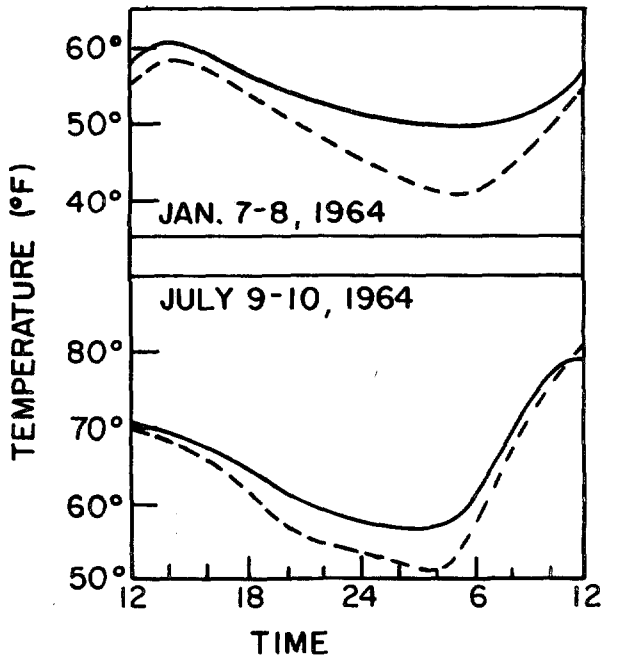

FIGURE 3.—Diurnal (LST) variation of the temperature in the city of San Francisco, Calif., (solid line) and at the airport (dashed line). These data have been filtered and corrected for height differential between measuring sites.

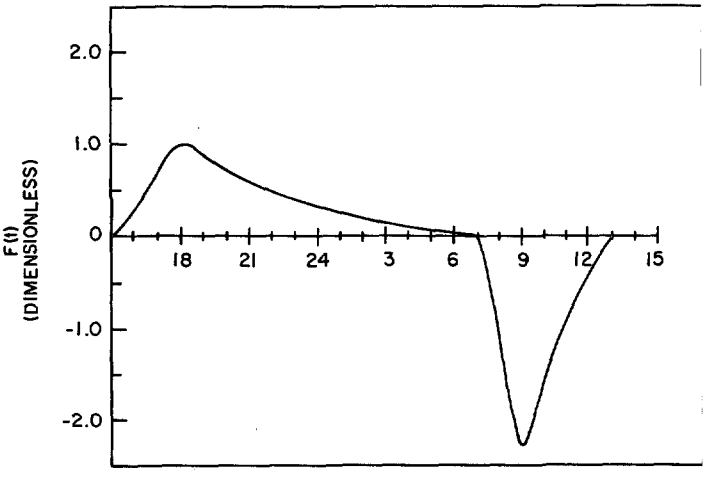

FIGURE 4.—The diurnal (LST) variation of the function $F(t)$. The values of $F(t)$ are based on the data presented in figure 1.

the city is warming. $F(t)$ is based on calculations made using the summer and winter Vienna data shown in figure 1 and is an average from the data. Similar curves were found for St. Louis and San Francisco. The positive differential heating is a maximum at 1800 LST and gradually decreases to zero just before sunrise. The negative differential heating attains a maximum value at 0900 LST and is zero at 1300 LST. During the period 1400–0600 LST, these results are reasonably consistent with those of Oke and East (1971) for Montreal except that their time of maximum positive differential heating was 2000 LST. They did not present data for 0600–1300 LST. The results are also consistent with those of Atwater (1971*b*).

The purpose of this study is to demonstrate the response of the atmosphere to the forcing function $F(t)$, the differential heating rate, which is assumed to be the only driving force. To achieve this end, we developed a simple, linear model to compute the diurnal variation of the vertical velocity in the center of the city. The differential heating distribution was assumed to take the form of a Gaussian distribution in the horizontal. The center of the city was assumed to be the point where the distribution was a maximum ($x=0$). The vertical distribution of the heating rate was assumed constant in the boundary layer and zero above the boundary layer in one case and was allowed to decay

exponentially with height through the boundary layer in another case. The stability in the boundary layer was also allowed to vary. In all cases, the synoptic wind speed was zero.

2. MODEL DEVELOPMENT

The heating and the motions were constrained to vary in the x-z plane. The forcing function was, therefore, infinitely long parallel to the y coordinate. The Coriolis force was neglected, and a linear friction term was employed. The linearized, perturbation equations of motion are

$$\left(\frac{\partial}{\partial t}+2K\right)u'=-\frac{1}{\bar{\rho}}\frac{\partial p'}{\partial x}$$

and

$$\left(\frac{\partial}{\partial t}+2K\right)w'=-\frac{1}{\bar{\rho}}\frac{\partial p'}{\partial z}-\frac{\rho'}{\bar{\rho}}g \tag{1}$$

where u' is the perturbation x component of the wind, w' is the perturbation vertical velocity, t is time, p' is the perturbation pressure, $\bar{\rho}$ is the average density independent of x and t, g is gravity, K is the coefficient of friction and is a constant, and ρ' is the perturbation density. Cross differentiation and subtraction of the equations of motion lead to the perturbation vorticity equation,

$$\left(\frac{\partial}{\partial t}+2K\right)\left(\frac{\partial u'}{\partial z}-\frac{\partial w'}{\partial x}\right)+\frac{\partial \beta}{\partial x}=0 \tag{2}$$

where $\beta=-g\rho'/\bar{\rho}=g\theta'/\bar{\theta}$. Here, θ' is the perturbation potential temperature, and $\bar{\theta}$ is the average potential temperature independent of x and t. Assuming nondivergence, we can find a stream function, ψ, such that

$$u'=\frac{\partial \psi}{\partial z} \text{ and } w'=-\frac{\partial \psi}{\partial x},$$

and eq (2) becomes

$$\left(\frac{\partial}{\partial t}+2K\right)\left(\frac{\partial^2\psi}{\partial z^2}+\frac{\partial^2\psi}{\partial x^2}\right)+\frac{\partial \beta}{\partial x}=0. \tag{3}$$

Scale analysis shows that the horizontal scale of the perturbation in the model is smaller than the vertical scale of the perturbation (i.e., $|\partial^2\psi/\partial z^2| >> |\partial^2\psi/\partial x^2|$); therefore, in a comparison of terms influenced by identical coefficients, $\partial^2\psi/\partial x^2$ may be neglected and eq (3) becomes

$$\left(\frac{\partial}{\partial t}+2K\right)\frac{\partial^2\psi}{\partial z^2}+\frac{\partial \beta}{\partial x}=0. \tag{4}$$

The first law of thermodynamics in linearized perturbation form is

$$\frac{\partial \beta}{\partial t}-\omega^2\frac{\partial \psi}{\partial x}=\lambda F(x)F(z)F(t) \tag{5}$$

where $\omega^2=(g/\bar{\theta})\,\partial\bar{\theta}/\partial z$, $\lambda=gQ'/c_{pa}\bar{T}$, Q' is the heating rate, $\bar{T}$ is the average temperature, c_{pa} is the specific heat at constant pressure, and $F(x)$, $F(z)$, and $F(t)$ are normalized functions that describe the variation of the heating in x, z, and t, respectively. $F(t)$ is given in figure 4. Eliminating β from eq (4) and (5) yields

$$\left(\frac{\partial^2}{\partial t^2}+2K\frac{\partial}{\partial t}\right)\frac{\partial^2\psi}{\partial z^2}+\omega^2\frac{\partial^2\psi}{\partial x^2}=-\lambda F_x(x)F(z)F(t) \tag{6}$$

where $F_x(x)=\partial F(x)/\partial x$.

Equation (6) is the governing equation that describes the motion. The solution was found by separation of variables subject to the boundary conditions

$$\psi=0,\ z=0,\ t\geq 0;$$
$$\psi=0,\ z=D,\ t\geq 0;$$

and

$$\psi=\frac{\partial \psi}{\partial t}=0,\ z\geq 0,\ t=0; \tag{7}$$

where D is the top of the atmosphere and acts as a rigid lid. Let

$$\lambda F(z)=\omega^2(z)\sum_n A_n\xi_n(z) \tag{8}$$

and

$$\psi=\sum_n f_n(x,\ t)\xi_n(z) \tag{9}$$

where the amplitude term, A_n, is

$$A_n=\lambda\int_0^D F(z)\xi_n(z)dz\left[\int_0^D \omega^2(z)\xi_n^2(z)dz\right]^{-1}, \tag{10}$$

n is the index used in the summation ($n=1,\ 2,\ 3,\ \ldots$), ξ_n and f_n are functions of z and of x and t, respectively, and are to be determined. Substituting eq (8) and (9) into eq (6) yields

$$\left(\frac{\partial^2}{\partial t^2}+2K\frac{\partial}{\partial t}-c_n^2\frac{\partial^2}{\partial x^2}\right)f_n=A_nc_n^2F_x(x)F(t), \tag{11}$$

and

$$\left(\frac{\partial^2}{\partial z^2}+\frac{\omega^2}{c_n^2}\right)\xi_n=0 \tag{12}$$

where c_n is the separation constant and is the internal gravity wave speed.

The forcing function is assumed to have a Gaussian distribution along the x axis. The functional form for this distribution was given by a Fourier series; that is,

$$F(x)=\exp(-\gamma x^2)=\sum_k a(k)\cos kx+b(k)\sin kx$$

where γ is the rate constant, k is the wave number, and $a(k)$ and $b(k)$ are Fourier coefficients. Under these conditions, a solution to eq (11) is

$$f_n(x,\ t)=\sum_k g(k,\ t)\cos kx+r(k,\ t)\sin kx, \tag{13}$$

provided

$$\left(\frac{\partial^2}{\partial t^2}+2K\frac{\partial}{\partial t}+c_n^2k^2\right)g=A_nkc_n^2b(k)F(t) \tag{14}$$

and

$$\left(\frac{\partial^2}{\partial t^2}+2K\frac{\partial}{\partial t}+c_n^2k^2\right)r=-A_nkc_n^2a(k)F(t). \tag{15}$$

Since the problem is linear, there is no loss of generality if we treat individual wave components as reflected in the above equations.

$F(t)$ is given in figure 4. However, the functional form used for $F(t)$ was also a Fourier series where the coefficients, $d(m)$ and $e(m)$, were determined using the data in the figure; that is,

$$F(t)=\sum_m d(m)\cos mt+e(m)\sin mt$$

where m is the wave number in the time domain. With this condition and the boundary conditions in eq (7), the solutions to eq (14) and (15) are

$$g(t,k)=A_n b(k)c_n F^*(t), \tag{16}$$

and

$$r(t,k)=-A_n a(k)c_n F^*(t), \tag{17}$$

where

$$F^*(t)=\sum_m\Bigg(\frac{d(m)\cos mt+e(m)\sin mt}{2\alpha}\Bigg\{\frac{\alpha+m}{(\alpha+m)^2+K^2}+\frac{\alpha-m}{(\alpha-m)^2+K^2}-e^{-Kt}\Bigg[\frac{K\sin(\alpha+m)t}{(\alpha+m)^2+K^2}+\frac{K\sin(\alpha-m)t}{(\alpha-m)^2+K^2}+\frac{(\alpha+m)\cos(\alpha+m)t}{(\alpha+m)^2+K^2}+\frac{(\alpha-m)\cos(\alpha-m)t}{(\alpha-m)^2+K^2}\Bigg]\Bigg\}$$

$$-\frac{e(m)\cos mt-d(m)\sin mt}{2\alpha}\times\Bigg\{K\Bigg[\frac{1}{(\alpha-m)^2+K^2}-\frac{1}{(\alpha+m)^2+K^2}\Bigg]+e^{-Kt}\Bigg[\frac{(\alpha-m)\sin(\alpha-m)t}{(\alpha-m)^2+K^2}-\frac{(\alpha+m)\sin(\alpha+m)t}{(\alpha+m)^2+K^2}-\frac{K\cos(\alpha-m)t}{(\alpha-m)^2+K^2}+\frac{K\cos(\alpha+m)t}{(\alpha+m)^2+K^2}\Bigg]\Bigg\}\Bigg)$$

and

$$\alpha=\sqrt{c_n^2k^2-K^2}.$$

The solution yields a forced response and a damped, transient response. The transient responses are internal gravity waves. As time increases, the transient response becomes negligible, and

$$F^*(t)=\sum_m\Bigg\{\Bigg[\frac{d(m)\cos mt+e(m)\sin mt}{2\alpha}\Bigg]\Bigg[\frac{\alpha+m}{(\alpha+m)^2+K^2}+\frac{(\alpha-m)}{(\alpha-m)^2+K^2}\Bigg]-K\Bigg[\frac{e(m)\cos mt-d(m)\sin mt}{2\alpha}\Bigg]\times\Bigg[\frac{1}{(\alpha-m)^2+K^2}-\frac{1}{(\alpha+m)^2+K^2}\Bigg]\Bigg\}$$

or

$$F^*(t)\propto F(t)-dF(t)$$

where $dF(t)$ is the change in $F(t)$ over an increment of time. The character of the forced response indicates that initially, when the heating is small and the rate of change of the heating is relatively large and positive, the forcing function could conceivably produce downward motion over the heated area until $F(t)$ becomes large. This appears similar to the effect apparent in the solutions of Estoque and Bhumralkar (1969) for the classical heat island when t is small.

The solution to eq (12) depends on ω, which varies in the vertical as $\bar{\theta}$ varies. The atmosphere was assumed to be characterized by three stability layers where ω is constant in each layer; that is,

$$\omega=\omega_1,\qquad 0\le z\le h_1,$$

$$\omega=\omega_2,\qquad h_1\le z\le h_2,$$

and

$$\omega=\omega_3,\qquad h_2\le z\le D.$$

Under these conditions, the solution that satisfies the boundary conditions [eq (7)] and the continuity conditions

$$\left.\begin{aligned}\xi_{1,n}&=\xi_{2,n}\\ \frac{\partial}{\partial z}\xi_{1,n}&=\frac{\partial}{\partial z}\xi_{2,n}\end{aligned}\right\}z=h_1$$

and

$$\left.\begin{aligned}\xi_{2,n}&=\xi_{3,n}\\ \frac{\partial}{\partial z}\xi_{2,n}&=\frac{\partial}{\partial z}\xi_{3,n}\end{aligned}\right\}z=h_2$$

is

$$\xi_{1,n}=\sin\frac{\omega_1 z}{c_n},\qquad 0\le z\le h_1$$

$$\xi_{2,n}=\sin\frac{\omega_1 h_1}{c_n}\cos\frac{\omega_2}{c_n}(z-h_1)+\frac{\omega_1}{\omega_2}\cos\frac{\omega_1 h_1}{c_n}\sin\frac{\omega_2}{c_n}(z-h_1),\qquad h_1\le z\le h_2$$

and (18)

$$\xi_{3,n}=\sin\frac{\omega_3}{c_n}(D-z)\sin^{-1}\frac{\omega_3}{c_n}(D-h_2)\Bigg[\sin\frac{\omega_1 h_1}{c_n}\cos\frac{\omega_2}{c_n}(h_2-h_1)+\frac{\omega_1}{\omega_2}\cos\frac{\omega_1 h_1}{c_n}\sin\frac{\omega_2}{c_n}(h_2-h_1)\Bigg],\qquad h_2\le z\le D$$

provided that

$$\frac{\omega_2}{c_n}-\frac{\omega_1}{c_n}\cot\frac{\omega_1 h_1}{c_n}\cot\frac{\omega_2}{c_n}(h_2-h_1)=\frac{\omega_3}{\omega_2}\cot\frac{\omega_3}{c_n}(D-h_2)\Bigg[\frac{\omega_2}{c_n}\cot\frac{\omega_2}{c_n}(h_2-h_1)-\frac{\omega_1}{c_n}\cot\frac{\omega_1 h_1}{c_n}\Bigg]. \tag{19}$$

The solution of eq (19) yields the eigenvalues, c_n. The expression for the amplitude term, A_n, will be given later. Equations (9), (10), (13), (16), (17), and (18) are combined to yield the time and space variations of the stream function, ψ. The vertical velocity is computed from the stream function, since $w'=-\partial\psi/\partial x$.

3. RESULTS

The heating decayed to essentially zero [$\exp(-\gamma x^2)=0.05$] at $x=\pm 10$ km for this study. The maximum excess temperature of 6°C occurred in the center of the city ($x=0$) at 0700 LST. This excess was reduced to zero by the differential cooling in the period 0700–1300 LST. The first kilometer was divided into two layers in which the temperature lapse rate was allowed to vary from case study to case study. The first layer was bounded by

$0 \leq z \leq h_1$ and $h_1 = 500$ m for all cases; the second layer is defined by $h_1 \leq z \leq h_2$ where $h_2 = 1.0$ km. In the third layer ($h_2 \leq z \leq D$), the temperature lapse rate was always equivalent to the standard atmospheric rate [$\Gamma = 6.5$°C/km], and $D = 10.0$ km. The coefficient of friction was 10^{-4}s^{-1}. The transient response became negligible in essentially 3.0 hr due to the friction.

Since the top of the urban boundary layer is found somewhere between 300 m and 1.0 km (Clarke 1969, Oke and East 1971), the heating was assumed constant in the layer $0 \leq z \leq h_1$ and zero above h_1; that is,

$$F(z) = H(h_1 - z),$$

where H is the Heaviside unit function. The amplitude term, A_m, was, therefore,

$$A_n = \frac{\lambda c_n}{\omega_1}\left(1 - \cos\frac{\omega_1 h_1}{c_n}\right)\delta^{-1}$$

where

$$\delta = \frac{\omega_1^2 h_1}{2} + \frac{\omega_2^2}{2}(h_2 - h_1)\sin^2\frac{\omega_1 h_1}{c_n} + \frac{\omega_1^2}{2}(h_2 - h_1)\cos^2\frac{\omega_1 h_1}{c_n}$$
$$+ c_n\omega_1 \cos\frac{\omega_1 h_1}{c_n}\sin\frac{\omega_1 h_1}{c_n}\sin^2\frac{\omega_2}{c_n}(h_2 - h_1) + \frac{\omega_3^2}{2}(D - h)$$
$$\times \sin^{-1}\frac{\omega_3}{c_n}(D - h_2)\left[\sin\frac{\omega_1 h_1}{c_n}\cos\frac{\omega_2}{c_n}(h_2 - h_1) + \frac{\omega_1}{\omega_2}\cos\frac{\omega_1 h_1}{c_n}\right.$$
$$\left.\times \sin\frac{\omega_2}{c_n}(h_2 - h_1)\right]^2.$$

Spatial Distribution of the Vertical Velocity

Figure 5 shows the spatial distribution of the vertical velocity for the steady-state solution. The lapse rate in the first layer ($0 \leq z \leq h_1$) was 6.5°C/km, and the second layer ($h_1 \leq z \leq h_2$) was isothermal. The atmospheric temperature profile is typical of conditions in the late morning hours. The differential heating rate is positive for this case and produces a 1°C temperature change in 1 hr. All other parameters are the same as given previously.

Upward vertical motion characterizes the center of the city. The layer of upward vertical motion is approximately 550 m thick. The horizontal boundaries of the upward motion are approximately $x = \pm 4.6$ km. The maximum vertical speed is 6.5 cm/s. The peripheral regions have downward motion, and the maximum downward speed is 2.4 cm/s. The asymmetry in the horizontal distribution of the vertical velocity is a result that differs from that found by Vukovich (1971) and occurs because the forcing function varies as exp $(-\gamma x^2)$ in this case and varied as the cos kx in the 1971 case. The distribution used here is probably more realistic.

Diurnal Variation of the Vertical Velocity

The solution under the conditions that the lapse rate in layer 1 is 6.5°C/km and in layer 2 is 8.0°C/km is given in figure 6. This stability profile is characteristic

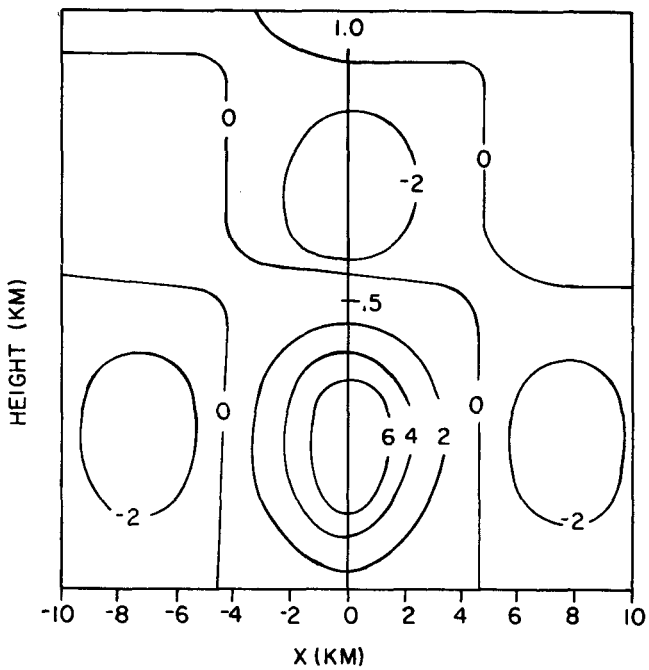

FIGURE 5.—The spatial variation of the vertical velocity (cm/s) due to the urban heat island. The lapse rate in layer 1 is 6.5°C/km and in layer 2 is 0.0°C/km. Heating is constant in the first 500 m and is zero above.

of late afternoon and early evening periods when the forcing function attains a maximum value. The solution is most valid in that time period. The heat island circulation is produced almost immediately. The maximum positive vertical speed is 4.1 cm/s, which compares favorably with the results of Angell et al. (1971). The observations of Angell et al. were made around 1900 LST, which is when the vertical velocity is a maximum in this case. The heat island circulation (positive vertical motion) was insignificant after 0200 LST. The top of the layer of positive vertical motion over the city was at about 540 m.

After 0730 LST, a layer (which is also 540-m thick) of downward motion developed over the city in response to the strong, negative differential heating. The circulation is thermally indirect because the city is still warmer than the suburbs. The maximum downward motion is greater than 8 cm/s, and occurs at 1000 LST, 1 hr after the minimum differential heating. Apparently, the difference in time between minimum vertical velocity and minimum differential heating is due to the stability in the boundary layer. The downward vertical motion ceased around 1300 LST.

A number of solutions with temperature profiles characteristic of different periods of the day were obtained. Instead of showing all these solutions, we picked from each solution those parts that are valid for a particular period of the day, depending on the stability, and grouped these into an overall solution. Table 1 shows the temperature lapse rates in each layer for each time period used for the overall solution (fig. 7). The definition of q in table 1 will be given later. If the diurnal variation of the vertical velocity for maximum temperature excesses different

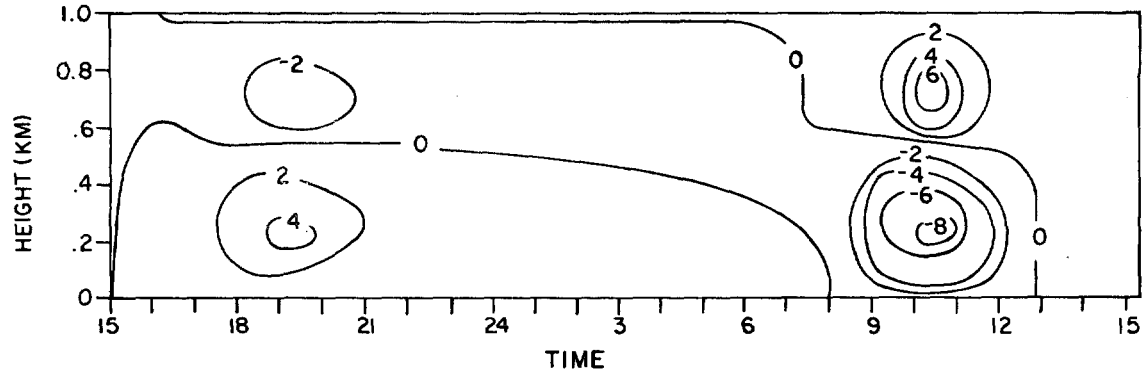

FIGURE 6.—The diurnal (LST) variation of the vertical velocity (cm/s) at the center of the city ($x=0$) due to the variations in the urban heat island given in figure 2. The lapse rate in layer 1 is 6.5°C/km and in layer 2 is 8.0°C/km. Heating is constant in the first 500 m and is zero above.

TABLE 1.—*The diurnal variation of the lapse rate in the three layers used in the computations*

Time period	Γ Layer 1	Γ Layer 2	Γ Layer 3	q
(LST)	(°C/km)	(°C/km)	(°C/km)	m^{-1}
1200 to 1800	8.0	8.0	6.5	0.0006
1800 to 2000	6.5	8.0	6.5	.0009
2000 to 0100	3.3	6.5	6.5	.0013
0100 to 0700	−2.5	3.3	6.5	.0019
0700 to 1000	6.5	0	6.5	.0013
1000 to 1200	8.0	6.5	6.5	.0009
1200 to 1300	8.0	8.0	6.5	.0006

from 6°C are desired, these may be obtained by multiplying the given vertical velocities by the ratio of the required maximum temperature excess to 6°C.

Initially (1600 LST), the vertical velocities of the heat island circulation develop through a comparatively deep layer (approximately 1.0 km) because of the relative instability in the boundary layer. The layer is quickly reduced to approximately 500 m as the stability increases near the surface. The vertical shrinking of the heat island circulation due to increasing stability has been discussed by Vukovich (1971). Because of the influence of the relatively unstable boundary layer at this time, the maximum vertical speed (8.0 m/s) occurs at 1700 LST, 1 hr before the forcing function is a maximum. After 2300 LST, the heat island circulation is negligible because of the increased stability.

Some time after sunrise, the urban boundary layer is characterized by intense downward vertical motion associated with a thermally indirect circulation produced in response to the negative differential heating. The maximum downward speed is greater than 18 cm/s and occurs at around 0900 LST, which is soon after the differential heating is a minimum. At this time, the top of the layer of downward motion is around 600 m. Around noon, however, it increases to 1.0 km in response to the decrease of stability in the boundary layer. The circulation ceases around 1300 LST.

The temperature profiles given to Oke and East (1971) indicate that, to a reasonable approximation, the temperature excess of the urban heat island decreases exponentially with height. This form of the vertical distribution of the differential heating was included in the model for the diurnal response by letting

$$F(z)=e^{-qz}H(h_2-z)$$

where q is the vertical rate constant. Heating decays exponentially with height through the first kilometer and is zero above. With this form for $F(z)$, the amplitude term, A_n, is

$$A_n=\lambda\left\{\frac{1}{\left(\frac{\omega_1}{c_n}\right)^2+q^2}\left[\frac{\omega_1}{c_n}-e^{-qh_1}\left(q\sin\frac{\omega_1 h_1}{c_n}+\frac{\omega_1}{c_n}\cos\frac{\omega_1 h_1}{c_n}\right)\right]\right.$$

$$+\frac{e^{-qh_1}}{\left(\frac{\omega_2}{c_n}\right)^2+q^2}\sin\frac{\omega_1 h_1}{c_n}\left[q-e^{-q(h_2-h_1)}\left(q\cos\frac{\omega_2}{c_n}(h_2-h_1)\right.\right.$$

$$\left.\left.-\frac{\omega_2}{c_n}\sin\frac{\omega_2}{c_n}(h_2-h_1)\right)\right]+\frac{\omega_1}{\omega_2}\cos\frac{\omega_1 h_1}{c_n}\left[\frac{\omega_2}{c_n}\right.$$

$$\left.\left.-e^{-q(h_2-h_1)}\left(q\sin\frac{\omega_2}{c_n}(h_2-h_1)+\frac{\omega_2}{c_n}\cos\frac{\omega_2}{c_n}(h_2-h_1)\right)\right]\right\}\delta^{-1}.$$

The rate constant, q, is a function of stability. Since the heating would occur through a relatively deep layer and rather uniformly in a relatively unstable boundary layer and would occur in a shallow layer in a relatively stable atmosphere, q would approach zero in the first case and would be relatively large in the second case. The variations of q with the stability conditions employed are shown in table 1. All other parameters remained the same as before. Only the overall solution determined from the stability categories listed in table 1 is shown (fig. 8).

A deep layer (approximately 2 km) of positive vertical motions developed in response to the positive heat differential. The maximum vertical velocity (approximately 10 cm/s) occurs at 1700 LST, 1 hr before the forcing function is a maximum. This again is due to the influence of stability. The urban heat island circulation is short-lived and the vertical velocities are negligible after 2000 LST. This, too, is primarily due to the influence of stability.

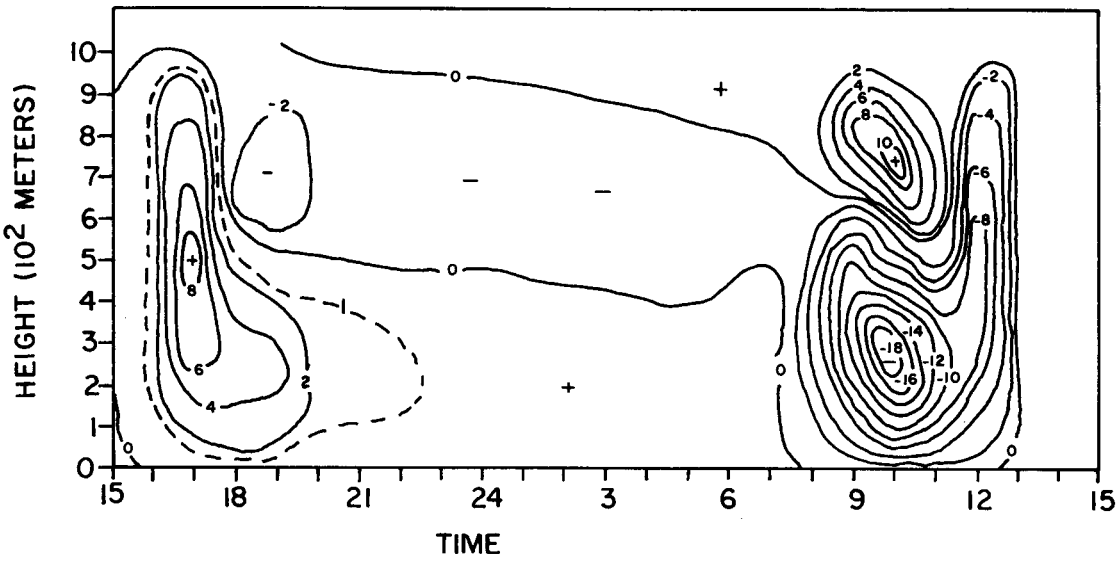

FIGURE 7.—The diurnal (LST) variation of the vertical velocity (cm/s) distribution at the center of the city ($x=0$) due to the variations in the urban heat island in figure 4. The heating was constant in the first 500 m and was zero above.

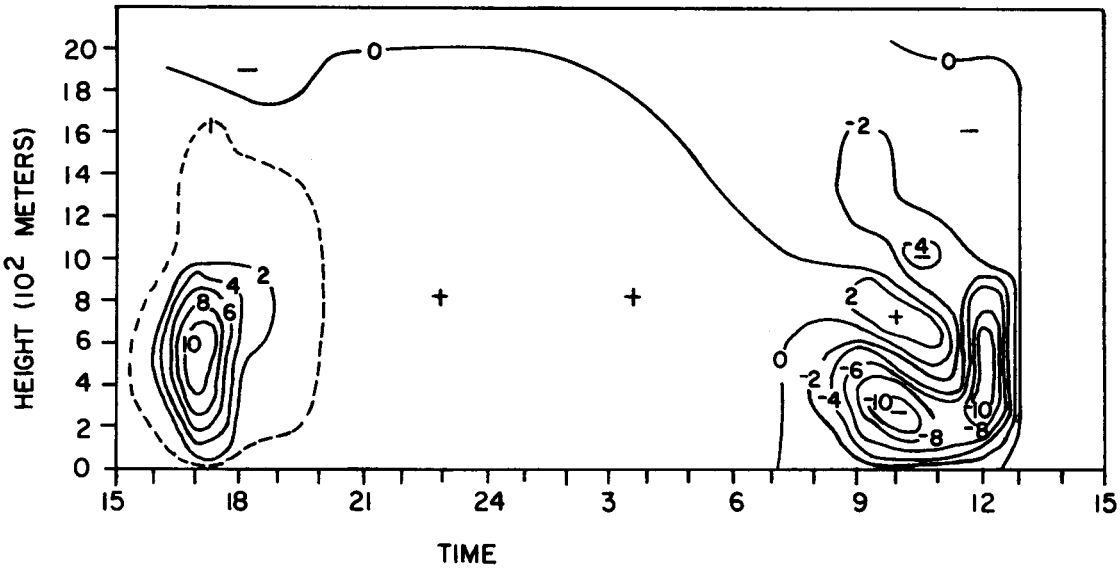

FIGURE 8.—The diurnal (LST) variation of the vertical velocity (cm/s) distribution at the center of the city ($x=0$) due to the variations in the urban heat island in figure 4. The heating decayed exponentially with height through the first kilometer and was zero above.

After sunrise, a relatively shallow layer (approximately 600 m) of downward vertical motion developed in response to the negative differential heating. The shallowness of the layer is apparently due to the upper stable layer. At around noon, the layer increased to 2 km in response to the decrease in stability in the boundary layer. The center of downward motion (−10 cm/s) found at 1000 LST is related to the amplitude of the forcing function at that time. The other center of equal magnitude occurring at noon is attributed to the decrease of stability in the boundary layer. The circulation ceases around 1300 LST.

The overall effect of having the forcing function decay exponentially with height, as opposed to being constant in the first 500 m as in the previous case, is to increase the depth and strength of the urban heat island circulation, to decrease the duration of the urban heat island circulation, and to decrease the intensity of the late-morning, thermally indirect circulation.

4. DISCUSSION OF RESULTS

The diurnal character of the temperature difference between a city and its surroundings, and therefore of the associated heat differential, is most often observed when the city is under the influence of a synoptic scale high-pressure system. A high-pressure system is usually characterized by weak winds and clear skies. The dynamic responses computed in the previous section are more likely to occur under these conditions. It is under these conditions that the so-called "critical episode" (with respect to air pollution and its effect on man) can occur.

The calculations presented in the previous section sug-

gest some interesting aspects concerning the transport of air pollutants under this synoptic condition and are specific for the no-mean-wind case. In the late afternoon and early evening, the weak urban heat island circulation slowly may lift the air pollution layer over the city. Since the vertical velocities are small, and the circulation is short-lived, the pollution layer would not be lifted much more than a few hundred meters. Somewhere between 2000 and 2300 LST, the urban heat island circulation, for all practical purposes, would cease because of the dampening due to the increase in the stability of the boundary layer. At this time, the pollution layer would become stagnant over the city.

After sunrise, the layer of air pollutants over the city inhibits solar radiation from reaching the surface in the city and, thus, rapid heating of the city does not occur. Since no such layer exists in the surrounding environment, the rural area heats up faster than the city. Under these conditions, negative differential heating is produced between the city and its suburbs, and a layer of downward motion may be created over the city in response to the forcing function. The magnitude of the vertical velocity in this case may be larger than that associated with the positive forcing function. The circulation would be thermally indirect.

As a consequence of this behavior, the air pollutants over the city would be transported to the surface. Furthermore, vertical diffusion of air pollutants from a surface source would be inhibited preventing rapid dilution. Since the period in which the downward motion would be created is usually the urban rush-hour period, large concentrations of air pollutants would be emitted at the surface. Collectively, these factors suggest that, in the late morning, large concentrations of air pollutants would be present at the surface leading possibly to an air pollution critical episode.

REFERENCES

Ackerman, Bernice, and Wormington, B., "Some Features of the Urban Heat Island," *Annual Report* ANL–7860, Radiological Physics Division, Argonne National Laboratory, Argonne, Ill., Dec. **1971**, pp. 183–192.

Angell, J. K., Pack, D. H., Dickson, C. R., and Hoecker, W. H., "Urban Influence on Nighttime Airflow Estimated From Tetroon Flights," *Journal of Applied Meteorology*, Vol. 10, No. 2, Apr. **1971**, pp. 194–204.

Atwater, Marshall A., "The Radiation Budget of Polluted Layers of the Urban Environment," *Journal of Applied Meteorology*, Vol. 10, No. 2, Apr. **1971***a*, pp. 205–214.

Atwater, Marshall A., "Thermal Effects of Pollutants Evaluated by a Numerical Model," *Proceedings of the 1st Conference on Air Pollution Meteorology, Raleigh, North Carolina, April 5–9, 1971*, American Meteorological Society, Boston, Mass., **1971***b*, pp. 108–113.

Chandler, T. J., "City Growth and Urban Climates," *Weather*, London, England, Vol. 19, No. 6, June **1964**, pp. 170–171.

Chandler, T. J., *The Climate of London*, Hutchinson & Co. London, England, **1965**, 292 pp.

Chandler, T. J., "London's Heat Island," *Biometeorology Part II: Proceedings of the 3rd International Biometeorological Congress, Pau, France, September 1–7, 1963*, Oxford, England, Pergamon Press, **1967**, pp. 589–597.

Clarke, John F., "Nocturnal Urban Boundary Layer Over Cincinnati, Ohio," *Monthly Weather Review*, Vol. 97, No. 8, Aug. **1969**, pp. 582–589.

Estoque, M. A., and Bhumralkar, C. M., "Flow Over a Localized Heat Source," *Monthly Weather Review*, Vol. 97, No. 12, Dec. **1969**, pp. 850–859.

Hage, Keith D., "Nocturnal Temperatures in Edmonton, Alberta," *Journal of Applied Meteorology*, Vol. 11, No. 1, Feb. **1972**, pp. 123–129.

Landsberg, Helmut E., "The Climate of Towns," *Proceedings of the International Symposium on Man's Role in Changing the Face of the Earth, Princeton, New Jersey, June 16–22, 1955*, University of Chicago Press, Chicago, Ill., **1956**, 584–606.

Lowry, William P., "The Climate of Cities," *Scientific American*, Vol. 217, No. 2, New York, N.Y., Aug. **1967**, pp. 15–32.

Ludwig, F. L., "Urban Climatological Studies," *Interim Report* No. 1, Contract No. OCD–PS–G4–201, Stanford Research Institute, Menlo Park, Calif., **1967**, 93 pp.

Mitchell, J. Murray Jr., "The Thermal Climate of Cities," *Symposium on Air Over Cities, Cincinnati, Ohio, November 6–7, 1961*, U.S. Public Health Service Report No. A62–5, Cincinnati, Ohio, Nov. **1961**, pp. 131–145.

Oke, T. R., and East C., "The Urban Boundary Layer in Montreal," *Boundary-Layer Meteorology*, D. Reidel Publishing Co., Dordrecht, Holland, Vol. 1, No. 4, Apr. **1971**, pp. 411–437.

Peterson, James T., "The Climate of Cities: A Survey of Recent Literature," *National Air Pollution Control Administration Publication* No. AP–59, Raleigh, N.C., Oct. **1969**, 48 pp.

Vukovich, Fred M., "Theoretical Analysis of the Effect of Mean Wind and Stability on a Heat Island Circulation Characteristic of an Urban Complex," *Monthly Weather Review*, Vol. 99, No. 12, Dec. **1971**, pp. 919–926.

Woollum, Clarence A., "Notes From a Study of the Microclimatology of the Washington, D.C. Area for the Winter and Spring Seasons," *Weatherwise*, Vol. 17, No. 6, Dec. **1964**, pp. 263–271.

Woollum, Clarence A., and Canfield, Norman L., "Washington Metropolitan Area Precipitation and Temperature Patterns," *ESSA Technical Memorandum*, WBTM–ER–28, U.S. Weather Bureau, Eastern Region, Garden City, N.Y., June **1968**, 8 pp.

[*Received March 2, 1973; revised May 18, 1973*]